JCI The Journal of Clinical Investigation

M-CSF mediates TNF-induced inflammatory osteolysis

Hideki Kitaura, … , F. Patrick Ross, Steven L. Teitelbaum

J Clin Invest. 2005;115(12):3418-3427. https://doi.org/10.1172/JCI26132.

Research Article **Bone biology**

TNF-α is the dominant cytokine in inflammatory osteolysis. Using mice whose BM stromal cells and osteoclast precursors are chimeric for the presence of TNF receptors, we found that both cell types mediated the cytokine's osteoclastogenic properties. The greater contribution was made, however, by stromal cells that express the osteoclastogenic cytokine M-CSF. TNF-α stimulated M-CSF gene expression, in vivo, only in the presence of TNF-responsive stromal cells. M-CSF, in turn, induced the key osteoclastogenic cytokine receptor, receptor activator of NF-κB (RANK), in osteoclast precursors. In keeping with the proproliferative and survival properties of M-CSF, TNF-α enhanced osteoclast precursor number only in the presence of stromal cells bearing TNF receptors. To determine the clinical relevance of these observations, we induced inflammatory arthritis in wild-type mice and treated them with a mAb directed against the M-CSF receptor, c-Fms. Anti–c-Fms mAb selectively and completely arrested the profound pathological osteoclastogenesis attending this condition, the significance of which is reflected by similar blunting of the in vivo bone resorption marker tartrate-resistant acid phosphatase 5b (TRACP 5b). Confirming that inhibition of the M-CSF signaling pathway targets TNF-α, anti–c-Fms also completely arrested osteolysis in TNF-injected mice with nominal effect on macrophage number. M-CSF and its receptor, c-Fms, therefore present as candidate therapeutic targets in states of inflammatory bone erosion.

M-CSF mediates TNF-induced inflammatory osteolysis

Hideki Kitaura,[1] Ping Zhou,[1] Hyun-Ju Kim,[1] Deborah V. Novack,[2] F. Patrick Ross,[1] and Steven L. Teitelbaum[1]

[1]Department of Pathology and [2]Department of Medicine, Washington University School of Medicine, St. Louis, Missouri, USA.

TNF-α is the dominant cytokine in inflammatory osteolysis. Using mice whose BM stromal cells and osteoclast precursors are chimeric for the presence of TNF receptors, we found that both cell types mediated the cytokine's osteoclastogenic properties. The greater contribution was made, however, by stromal cells that express the osteoclastogenic cytokine M-CSF. TNF-α stimulated M-CSF gene expression, in vivo, only in the presence of TNF-responsive stromal cells. M-CSF, in turn, induced the key osteoclastogenic cytokine receptor, receptor activator of NF-κB (RANK), in osteoclast precursors. In keeping with the proproliferative and survival properties of M-CSF, TNF-α enhanced osteoclast precursor number only in the presence of stromal cells bearing TNF receptors. To determine the clinical relevance of these observations, we induced inflammatory arthritis in wild-type mice and treated them with a mAb directed against the M-CSF receptor, c-Fms. Anti–c-Fms mAb selectively and completely arrested the profound pathological osteoclastogenesis attending this condition, the significance of which is reflected by similar blunting of the in vivo bone resorption marker tartrate-resistant acid phosphatase 5b (TRACP 5b). Confirming that inhibition of the M-CSF signaling pathway targets TNF-α, anti–c-Fms also completely arrested osteolysis in TNF-injected mice with nominal effect on macrophage number. M-CSF and its receptor, c-Fms, therefore present as candidate therapeutic targets in states of inflammatory bone erosion.

Introduction

Inflammatory osteolysis attends disorders such as rheumatoid and psoriatic arthritis, which are among the most crippling of skeletal diseases. In this circumstance, osteoclasts erode periarticular bone, leading to joint collapse and disfigurement. The fact that large numbers of such osteoclasts appear juxtaposed to foci of synovitis suggests that the products of inflammation mediate cell recruitment.

Osteoclasts have the unique capacity to resorb bone and are derived from monocyte/macrophage precursors (1). The discovery that receptor activator of NF-κB ligand (RANKL) is the specific osteoclastogenic cytokine (2, 3) led to the development of techniques whereby pure populations of osteoclasts can be generated in culture and eventuated in targeted, antiresorptive therapeutic strategies (4).

Other cytokines, however, also have a significant impact on the osteoclastogenic process, not least of which is TNF-α. This molecule, which is produced in abundance in bone erosive diseases such as rheumatoid arthritis and periodontitis (5–9), profoundly accelerates the osteoclastogenic process (10). Interestingly, TNF-α alone is not sufficient to promote osteoclast precursor differentiation but has an impact only on cells simultaneously stimulated, or primed, with RANKL (10). Thus, inflammatory osteolysis does not occur in RANK-deficient mice (11, 12).

The discovery that TNF-α is central to the bone loss attending inflammation led to the development of agents that specifically block the cytokine and thus arrest the resorptive process (13). Anti-TNF therapy is not without complication, however, as patients are prone to infections, likely reflecting immune suppression. In addition, it appears that targeting of inflammatory cytokines such as TNF-α and IL-1 in combination is substantially more effective than suppression of only 1 (14). Thus, detailing the panoply of cytokines that mediate inflammatory osteolysis carries therapeutic implications.

Osteoclastogenesis requires participation of both osteoclast precursors, principally in the form of BM macrophages (BMMs), and BM stromal cells and their derivative osteoblasts. In general, pro-osteoclastogenic agents target BM stromal cells, which are the source of RANKL. RANKL, in turn, activates its receptor on BMMs, prompting them to assume the osteoclast phenotype. TNF-α exerts its osteoclastogenic effect by stimulating stromal cells to produce RANKL but, at high doses, also directly activates the osteoclast precursor (15).

Given that both osteoclast precursors and stromal cells are TNF-α targets, we determined their relative contributions to inflammatory osteoclastogenesis. We found that while the presence of the cytokine receptor on either cell type was sufficient to promote some degree of TNF-α–induced osteoclastogenesis, stromal cells made the greater contribution. Furthermore, TNF-α induces in vivo expression of the stromal cell product M-CSF, which maintains survival and longevity of osteoclast precursors and organizes the cytoskeleton of the mature resorptive cell (16). The fact that M-CSF plays a central role in TNF-induced osteoclastogenesis is confirmed by the capacity of an antibody directed against the M-CSF receptor, c-Fms, to completely arrest pathological osteoclastogenesis and bone resorption, whether attending inflammatory arthritis or direct injection of TNF-α. M-CSF and its receptor, c-Fms, are therefore candidate therapeutic targets for inflammatory osteolysis.

Nonstandard abbreviations used: BMM, bone marrow macrophage; IL-1Ra, IL-1 receptor antagonist; MTT, 3-[4,5-dimethylthiazol-2yl]-2,5-diphenyltetrazoliun bromide; RANK, receptor activator of NF-κB; RANKL, RANK ligand; TNFR, TNF receptor; TRACP 5b, tartrate-resistant acid phosphatase 5b; TRAP, tartrate-resistant acid phosphatase.

Conflict of interest: The authors have declared that no conflict of interest exists.

Citation for this article: *J. Clin. Invest.* **115**:3418–3427 (2005). doi:10.1172/JCI26132.

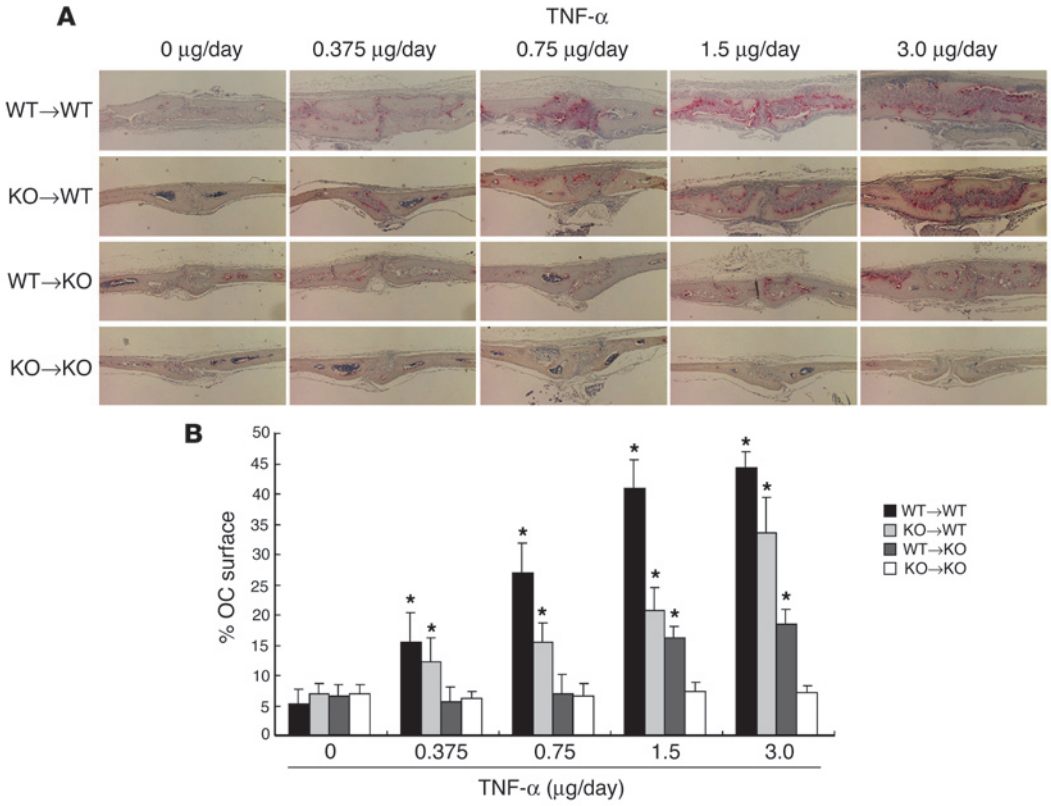

Figure 1
Macrophage and stromal cell responsivity to TNF-α are required for optimal TNF-α–induced osteoclastogenesis in vivo. (**A**) Histological sections of calvaria excised from WT to WT (WT→WT), WT to KO, KO to WT, and KO to KO mice after 5 daily supracalvarial injections of increasing doses of TNF-α were stained for TRAP activity (red reaction product). Magnification, ×40. (**B**) The percentage of BM interface covered by osteoclasts was histomorphometrically determined in specimens derived from WT to WT, KO to WT, WT to KO, and KO to KO mice. *$P < 0.01$ compared with KO to KO mice. $n = 3$ mice per group.

Results

BM stromal cells and osteoclast precursors contribute to TNF-induced osteoclastogenesis in vivo. We have shown that both BM stromal cells and osteoclast precursors are direct targets of TNF-α in the osteoclastogenic process (10, 15). The goal of our first exercise was, therefore, to determine the relative contributions of each. To this end, we turned to chimeric mice in which either WT or p55/p75 *TNF receptor–deficient* (*TNFR*$^{-/-}$) BM was transplanted into irradiated recipients bearing the same or reciprocal genotype. T cells were eliminated in vivo during the course of the experiment by injection of anti-CD4 and anti-CD8 mAbs (15). Thus, WT BM transplanted into irradiated *TNFR*$^{-/-}$ (WT to KO) mice serves as a model in which osteoclast precursors but not BM stromal cells express TNFRs whereas the opposite obtains in KO to WT chimeras. WT to WT and KO to KO irradiated and transplanted animals were used as positive and negative controls, respectively.

Validating the chimeric transplantation model, BMMs isolated from WT to KO mice expressed both TNFRs in quantities similar to their WT to WT counterparts (Supplemental Figure 1; available online with this article; doi:10.1172/JCI26132DS1). Similarly, macrophages derived from KO to WT mice were identical in this regard to those of animals lacking receptors on both cell types (KO to KO).

Each group of chimeric mice was subjected to daily supracalvarial administration of increasing doses of TNF-α. The animals were sacrificed on day 5, histological sections of the calvaria were stained for tartrate-resistant acid phosphatase (TRAP) activity, and osteoclast number was determined (Figure 1). As expected, KO to KO animals failed to respond to the cytokine while WT to WT animals generated osteoclasts in a dose-dependent manner. A similarly progressive albeit more modest increase in osteoclast number occurred in mice in which TNFRs were absent in osteoclast precursors (KO to WT). The response to the cytokine was, however, substantially more blunted in chimeras lacking stromal cell TNFRs. Thus, while the presence of TNFRs on either stromal cells or osteoclast precursors was sufficient to promote some degree of osteoclastogenesis, optimal osteoclast recruitment required expression of the receptor by both cell types with the greater contribution made by stromal cells.

TNF-α impacts the RANK/RANKL axis. Because the RANK/RANKL axis is central to osteoclast recruitment, we asked if it is differentially impacted in the various chimeric mice (Figure 2A). Thus, we administered TNF-α or carrier for 5 days and assayed BM for both RANKL and its receptor. As we have shown, TNF-α induces RANKL gene expression in WT to WT but not in KO to KO mice (15). In keeping with their greater contribution to TNF-α–stimulated osteoclastogenesis, TNFRs on stromal cells, but not preosteoclasts, were necessary for RANKL induction by the cytokine. On the other hand, *RANK* mRNA levels were equivalent whether osteoclast precursors, stromal cells, or both express TNFRs. Thus, whereas RANKL induction by TNF-α required direct targeting of stromal cells, *RANK* mRNA expression by BMMs may have been stimulated directly (WT to KO) or indirectly (KO to WT) by the cytokine.

M-CSF mediates TNF-induced osteoclastogenesis. To determine the mechanism by which TNF-α simulates RANK via a stromal cell–dependent mechanism, we turned to another stromal cell–produced osteoclastogenic cytokine, namely M-CSF, and asked if the growth factor promotes *RANK* mRNA expression by BMMs. In fact, like TNF-α, M-CSF induced RANK gene expression in a dose-dependent fashion (Figure 2B). Therefore, the indirect stimulatory effect of TNF-α on *RANK* mRNA expression may be mediated by stromal cell induction of M-CSF.

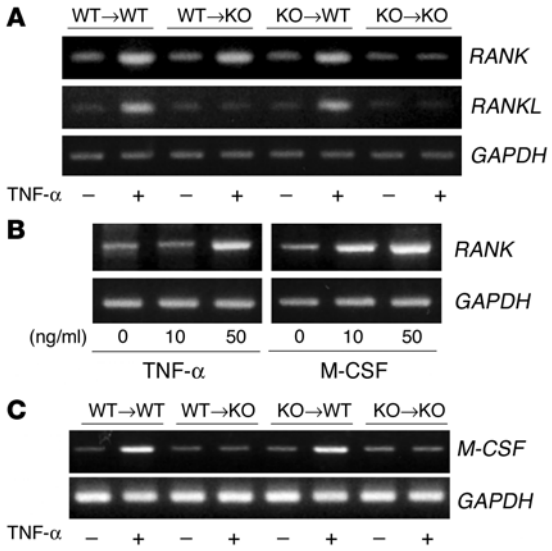

Figure 2
(**A**) TNF-α increases *RANK* mRNA expression in vivo. BM was obtained from WT to WT, WT to KO, KO to WT, and KO to KO mice after 5 daily injections of TNF-α (3 μg/day) or vehicle. RNA was isolated, and *RANK* and *RANKL* mRNA expression was measured by RT-PCR. *GAPDH* mRNA served as loading control. (**B**). TNF-α and M-CSF increase *RANK* mRNA expression in vitro. WT BMMs were cultured without M-CSF. After 24 hours, the cells were placed in medium containing increasing amounts of TNF-α or M-CSF. Six hours later, RNA was isolated and *RANK* mRNA expression was measured by RT-PCR. *GAPDH* mRNA served as loading control. (**C**) TNF-α increases *M-CSF* mRNA expression in vivo. BM was obtained from WT to WT, WT to KO, KO to WT, and KO to KO mice after 5 daily injections of TNF-α (3 μg/day) or vehicle. RNA was isolated, and *M-CSF* mRNA expression was measured by RT-PCR. *GAPDH* mRNA served as loading control.

To further explore this issue, we asked if TNF-α induces M-CSF expression in vivo in a stromal cell–dependent fashion. We therefore injected TNF-α into the 4 chimeric species of mice for 5 days, after which we assessed BM *M-CSF* mRNA levels. TNF-α induced *M-CSF* mRNA in WT to WT and KO to WT but not in WT to KO or KO to KO mice (Figure 2C). Hence, the capacity of TNF-α to stimulate M-CSF gene expression requires the presence of cytokine-responsive stromal cells.

M-CSF promotes osteoclastogenesis by stimulating proliferation and survival of osteoclast precursors (17). If M-CSF represents a means by which TNF-α indirectly promotes osteoclast recruitment, one would expect absence of TNFRs on stromal cells to dampen osteoclast precursor number. In this regard, TNF-α administered to mice increased the percentage of BM cells expressing the macrophage marker CD11b (Figure 3). Furthermore, TNF-α–mediated enhancement of osteoclast precursor number required the cytokine receptor only on stromal cells, a source of M-CSF.

TNF-α enhancement of osteoclast precursor number is not mediated by IL-1. TNF-α–induced osteoclastogenesis reflects both IL-1–dependent and –independent mechanisms (18). The IL-1 mediated event, while involving BMMs, also participates in the effect of TNF-α on stromal cells and has the capacity to directly induce RANKL expression (18). This observation raises the possibility that TNF-α–stimulated M-CSF production, and thus enhancement of osteoclast precursor number, is mediated via IL-1. To address this issue, we used a VCAM-1 affinity column to isolate BM stromal cells from WT mice and those deleted of IL-1RI (18). The cells were then exposed to TNF-α or IL-1-α. As seen in Figure 4, TNF-α, but not IL-1-α, induced M-CSF gene expression in WT stromal cells, and the effect was not impacted by IL-1 receptor antagonist (IL-1Ra). The fact that IL-1 did not mediate TNF-α induction of M-CSF mRNA is further confirmed by the lack of impact of IL-1RI deletion. Again consistent with stimulated M-CSF synthesis, TNF-α enhancement of osteoclast precursor number in vivo was unaltered in mice lacking IL-1-α or its receptor (Figure 5).

Stromal cells or BMMs mediate optimal inflammatory osteolysis. We have shown that the presence of TNFRs solely on osteoclast precursors is sufficient to optimize bone loss in inflammatory arthritis (15). On the other hand, stromal cells are the source of TNF-α–induced M-CSF, and we therefore asked if the same occurs only if they express TNFRs. Thus, arthrogenic serum or PBS was administered to the 4 species of chimeric mice (19, 20). By 7 days, all developed cutaneous inflammation (Figure 6A). Paw swelling was also present in each, which, while identical in the 3 species of TNFR-bearing animals, was substantially less in KO to KO

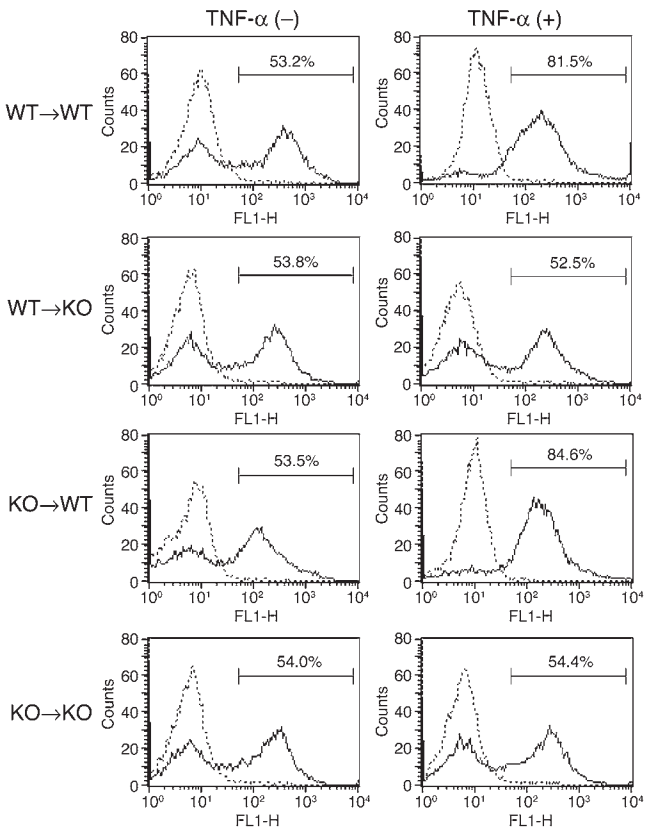

Figure 3
TNF-α–mediated increase in osteoclast precursor number in vivo requires cytokine-responsive stromal cells. The percentage of osteoclast precursors in BM recovered from WT to WT, WT to KO, KO to WT, and KO to KO mice after 5 daily injections of TNF-α (3 μg/day) or vehicle was determined by FACS, using FITC-conjugated anti-CD11b mAb (solid line) and FITC-conjugated isotype mAb (dotted line).

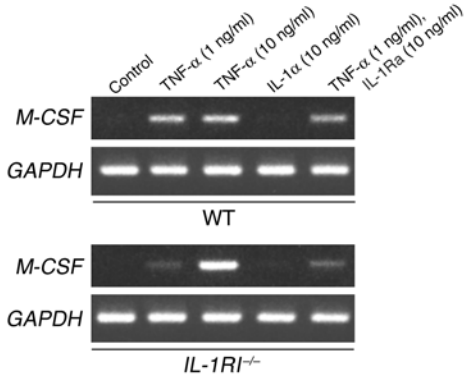

Figure 4
TNF-α induces *M-CSF* mRNA expression by BM stromal cells independent of IL-1. BM stromal cells were isolated on a VCAM-1 affinity column from WT or *IL-1RI*$^{-/-}$ mice. VCAM-1–positive cells were then exposed to carrier (control) or TNF-α, IL-1α, and IL-1Ra alone or in combination for 24 hours. *M-CSF* mRNA in equal amounts of total RNA was determined by RT-PCR. *GAPDH* mRNA served as loading control.

mice (Figure 6B). Whereas periarticular inflammation was extensive in the WT to WT, WT to KO, and KO to WT serum-injected mice, it was sparse in those devoid of TNFRs (Figure 6C). Importantly, inflammatory osteolysis, as manifested by the percentage of bone surface juxtaposed to osteoclasts, was indistinguishable in arthritic mice whether TNFRs were present on stromal cells, preosteoclasts, or both (Figure 6, D and E). In contrast, no significant osteoclastogenesis obtained in serum-injected KO to KO mice or any species administered PBS. Finally, osteoclast precursor number, represented by CD11B expression, was also enhanced to similar degrees in the BM of the 3 TNFR-bearing chimeras (Figure 7). These observations are in keeping with the hypothesis that, in the context of severe inflammation, TNF-α enhances osteoclast precursor number by stimulating stromal cell production of M-CSF (KO to WT) or acting in concert with constitutive levels of the latter cytokine (WT to KO).

Blockade of M-CSF–induced signaling prevents inflammatory osteolysis. The data presented thus far raise the possibility that M-CSF plays a central role in states of TNF-α–induced osteolysis, including inflammatory arthritis. To explore the clinical implications of this issue, we turned to a mAb generated against the M-CSF receptor, c-Fms (21). To determine its efficacy, we added increasing amounts of the antibody to cultures of WT BMMs in the presence of M-CSF alone or induced to undergo osteoclastogenesis by M-CSF and RANKL. After 3 days, we determined the number of BMMs and osteoclasts, respectively. Figure 8 shows that substantial osteoclast arrest occurred relative to control (0 ng/ml) at a dose (10 ng/ml) of the antibody at least 1 order of magnitude lower than that impacting macrophage number (100 ng/ml).

This observation prompted us to assess the effect of the anti–c-Fms mAb in inflammatory arthritis. Thus, WT mice administered arthrogenic serum received daily injections of anti–c-Fms mAb or PBS. Nonarthritic animals received only PBS. Seven days later, cutaneous inflammation (Figure 9A) and paw thickness (Figure 9B) of mice treated with the antibody or PBS were indistinguishable. Histological examination of the ankles confirmed the abundance of inflammation in each and its absence in nonarthritic animals (Figure 9C). As expected, those serum-treated animals receiving PBS underwent extensive osteoclastogenesis with bone resorptive cells juxtaposed to virtually the entire inflamed bone surface (Figure 9, C and D). On the other hand, antibody-treated mice exhibited a total arrest of arthritis-induced osteoclastogenesis despite persistence of profound inflammation.

In keeping with the clinical implications of these observations, the increase in bone resorptive activity induced by inflammatory arthritis was completely prevented in antibody-treated animals (Figure 9E). Despite a small but significant decrease in serum tartrate-resistant acid phosphatase 5b (TRACP 5b) levels in arthritic mice receiving anti–c-Fms as compared with naive animals, the antibody appeared to exert a substantially greater impact on inflammation-induced than physiological osteoclastogenesis, as TRAP-expressing cells within the tibial metaphysis appeared to be abundant in each circumstance (Figure 9F).

Although TNF-α is a dominant mediator, the osteoclastogenesis of inflammatory arthritis is the product of a number of cytokines. Therefore, as a final exercise, we asked if arrest of M-CSF signaling specifically affects TNF-α–stimulated bone resorption. WT mice were administered supracalvarial TNF-α daily, with or without anti–c-Fms mAb. Once again, control animals received only PBS. By 5 days, TNF-α alone induced a marked osteoclastogenic response, which was completely prevented by c-Fms mAb (Figure 10, A and B). Similar to animals with inflammatory arthritis, this arrest of TNF-α–induced osteoclastogenesis was paralleled by blunting of in vivo bone resorption manifested by TRACP 5b serum to a level even lower than that of controls (Figure 10C). Again reflecting the relative sensitivity of osteoclast recruitment as compared with precursor number to anti–c-Fms, the antibody only nominally affected the number of CD11B cells

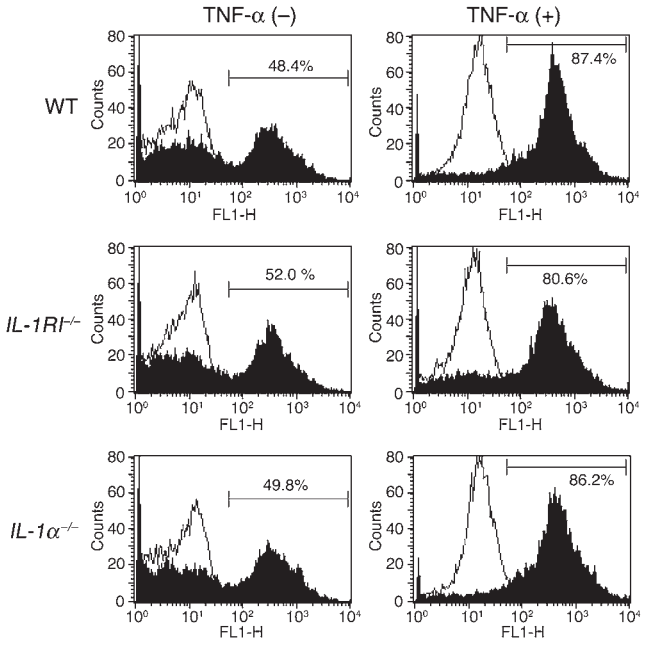

Figure 5
TNF-α–mediated increase in osteoclast precursor number in vivo is IL-1 independent. The percentage of osteoclast precursors in BM recovered from WT, *IL-1RI*$^{-/-}$, and *IL-1α*$^{-/-}$ mice after 5 daily injections of TNF-α (3 μg/day) or vehicle was determined by FACS using FITC-conjugated anti-CD11b mAb (filled profiles) and FITC-conjugated isotype mAb (open profiles).

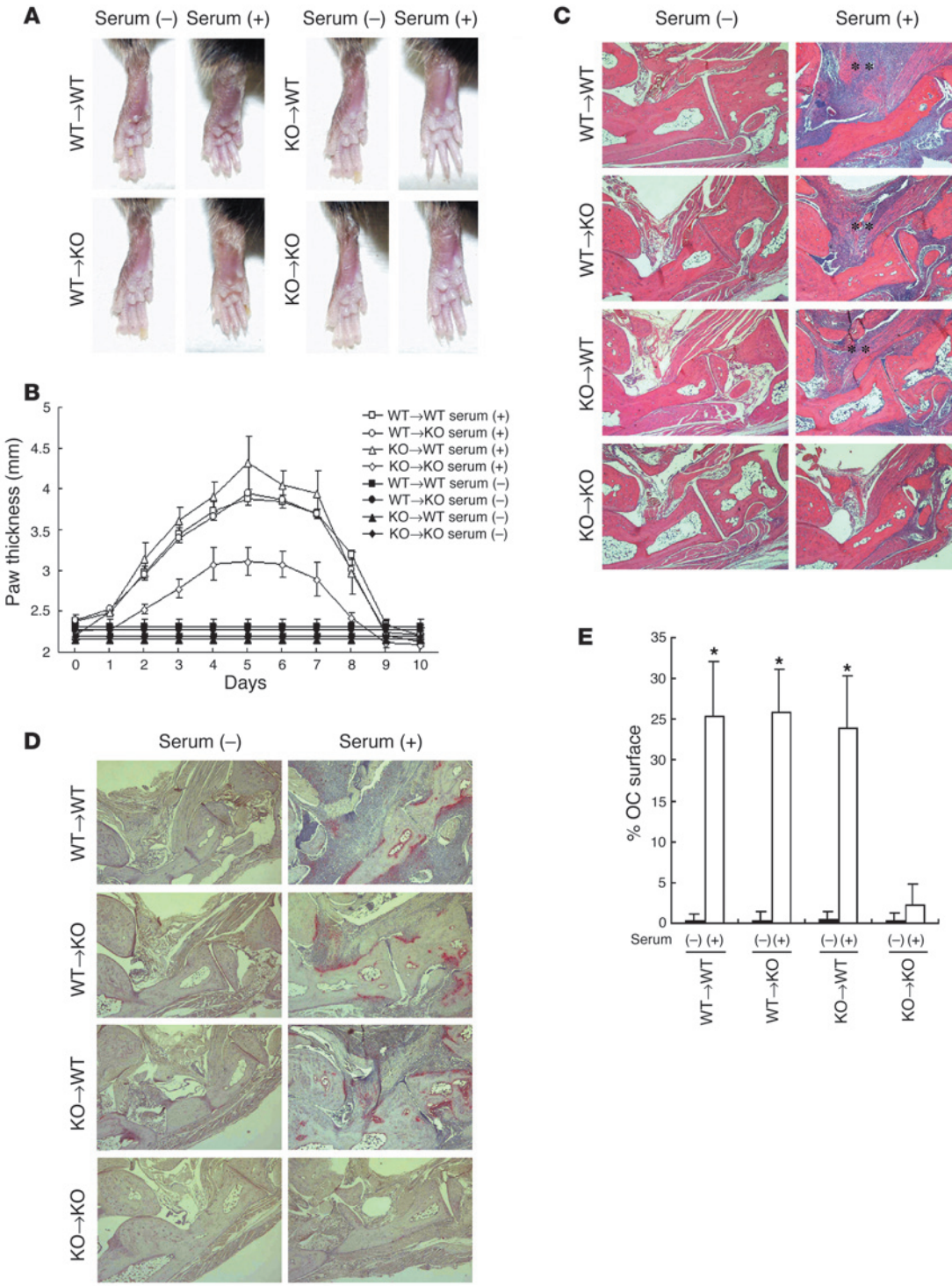

Figure 6
Stromal cells or BMMs mediate optimal inflammatory osteolysis. Mice in each chimeric group were injected with arthrogenic serum derived from K/BxN mice. (**A**) Appearance of paws of representative mice at day 7 after injection with arthrogenic serum (+) or PBS (–). (**B**) Paw thickness measured daily for 10 days for each group of chimeric mice injected with arthrogenic serum (+) or PBS (–). (**C**) H&E-stained histological sections of ankles at day 7 showing severe inflammation (**) in arthrogenic serum-treated (+) WT to WT, WT to KO, and KO to WT mice compared with the relatively mild changes occurring in similarly treated KO to KO animals. Minus sign indicates those injected with PBS. (**D**) TRAP-stained histological sections of ankles of serum-injected or serum-noninjected WT to WT, WT to KO, KO to WT, and KO to KO mice at day 7. (**E**) Histomorphometric quantitation of the percentage of bone surface covered by osteoclasts (OC) in ankles of PBS-treated (–) or arthrogenic serum–treated (+) WT to WT, WT to KO, KO to WT, and KO to KO mice.*$P < 0.001$ arthrogenic serum– vs. PBS-treated mice. $n = 4$ mice per group. Magnification, ×40.

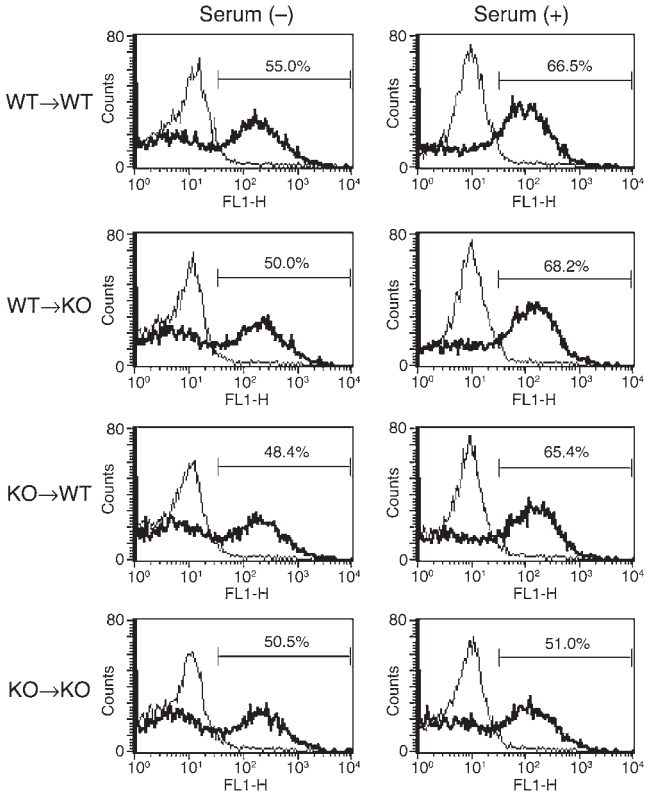

Figure 7
Stromal cells or BMMs mediate optimal inflammation-induced osteoclast precursor number. The percentage of osteoclast precursors in BM recovered from WT to WT, WT to KO, KO to WT, and KO to KO mice 7 days after injections of arthrogenic serum or vehicle was determined by FACS using FITC-conjugated anti-CD11b mAb (thick lines) and FITC-conjugated isotype mAb (thin lines).

in TNF-α–treated mice (70.7% ± 0.6% vs. 90.2% ± 2.0% of isolated BM cells) (Figure 10D).

Discussion

Rheumatoid arthritis is a complicated condition, as a host of cytokines produced by a variety of cells contributes to its pathogenesis. While RANKL and IL-1 are important participants in development of focal bone erosions, which eventuate in joint collapse, TNF-α is the principal and rate-limiting culprit, as its blockade dampens both the inflammatory and osteoclastogenic components of the disease (13). On the other hand, blockade of TNF-α alone is insufficient to optimize arrest of inflammatory joint disease, as coordinate treatment with IL-1Ra is more effective (14). Added to the potential complications attending TNF-α inhibition, these observations underscore the importance of identifying new therapeutic candidates in this disease, a goal which can be achieved only by gaining insight into the means by which TNF-α impacts its target cells.

Inflammatory osteoclastogenesis represents a complex relationship between macrophages and mesenchymal stromal cells, including those in BM and synovium. Each produce, and are targets of, inflammatory cytokines such as TNF-α, which enhances osteoclastogenesis by impacting both families of cells (15, 18). The cytokine stimulates stromal cells to synthesize RANKL and IL-1. TNF-α also directly prompts macrophages to differentiate into osteoclasts when exposed to constitutive levels of the key osteoclastogenic cytokine, i.e., RANKL (10). Thus, our first exercise was to determine the relative contributions of stromal cells and macrophages to TNF-α–induced osteoclastogenesis. Because this undertaking required isolating the contribution of each in vivo, we turned to mice chimeric for TNFRs in the BM and stromal compartment and found that, while both were required for optimal TNF-α–induced osteoclastogenesis, stromal cells had the greater impact. This pronounced contribution of stromal cells to the osteoclastogenic process involved stimulated production of RANKL. Alternatively, TNF-α–induced *RANK* mRNA levels in osteoclast precursors were similar whether TNFRs were present on macrophages, stromal cells, or both. Thus, enhanced RANK expression does not account for the dominant role played by stromal cells in TNF-α-stimulated osteoclast recruitment.

RANKL and IL-1 are produced by stromal cells under the influence of TNF-α, but the importance of these cells as indi-

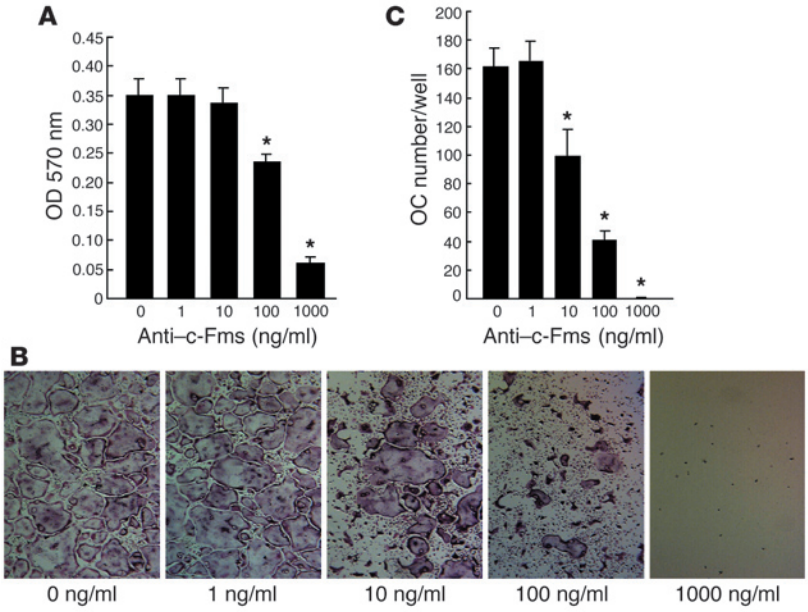

Figure 8
Anti–c-Fms antibody arrests osteoclastogenesis in vitro. (**A**) BMMs from WT mice were cultured with increasing amounts of anti–c-Fms mAb in the presence of 100 ng/ml M-CSF. After 3 days, the number of viable cells was measured using the MTT assay. MTT absorbance was determined at an OD of 570 nm. (**B**) The same number of BMMs were cultured in the presence of M-CSF (100 ng/ml) and RANKL (50 ng/ml) with increasing amounts of anti–c-Fms mAb for 3 days. The cells were stained for TRAP activity to identify osteoclasts. Magnification, ×400. (**C**) Number of osteoclasts generated in wells containing various amounts of anti–c-Fms antibody. *P < 0.001 vs. 0 ng/ml.

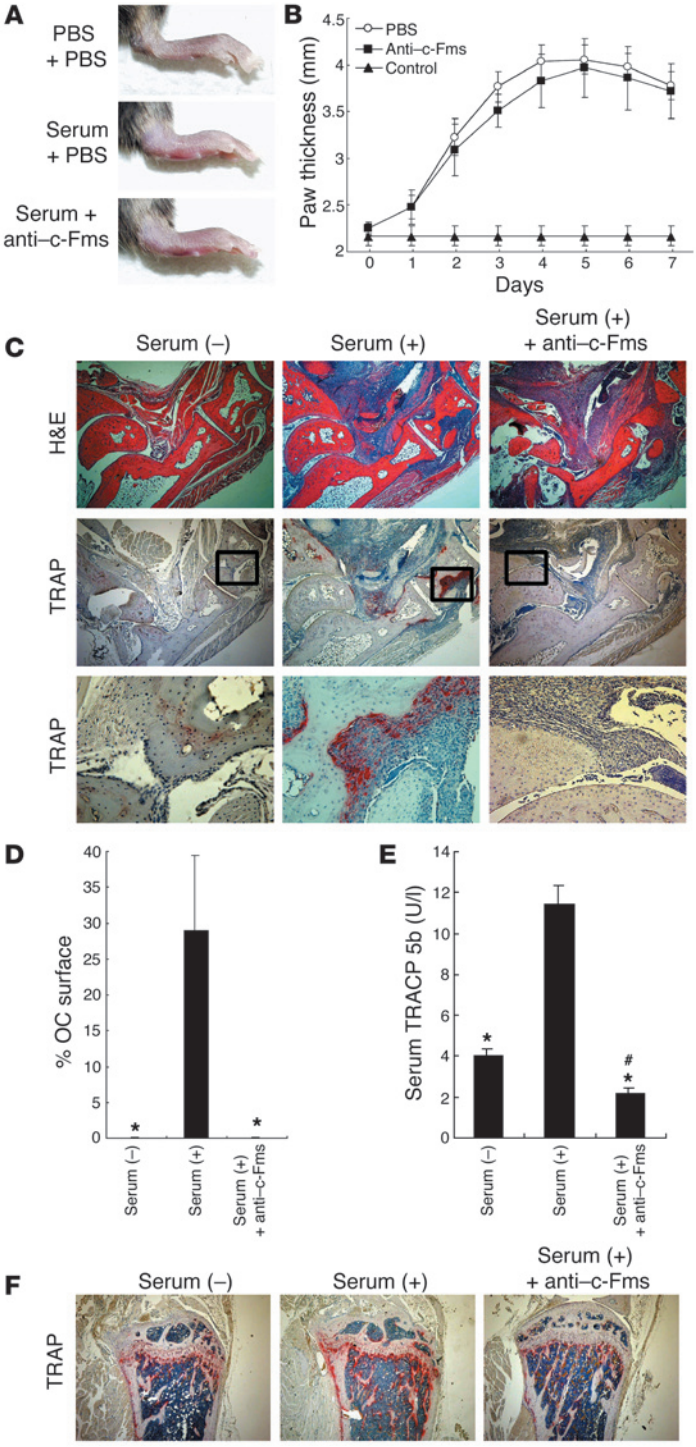

Figure 9
Anti–c-Fms mAb blocks inflammatory arthritis–induced osteoclastogenesis and bone resorption in vivo. Mice were injected with arthrogenic serum with or without daily administration of anti–c-Fms mAb or PBS. (**A**) Appearance of paws of representative mice at 7 days after injection with arthrogenic serum with or without anti–c-Fms mAb. (**B**) Paw thickness, measured daily for 7 days. (**C**) H&E- or TRAP- stained histological sections of ankles at day 7. TRAP reaction product identifying osteoclasts is red. Bottom panels are detailed views of boxed-in areas in middle panels. Magnification: ×40 (top and middle panels), ×200 (bottom panels). (**D**) Histomorphometric quantitation of the percentage of bone surface covered by osteoclasts in ankles of each group of mice. (**E**) Circulating TRACP 5b levels. (**F**). Representative TRAP-stained histological sections of proximal tibia of each group of mice. TRAP reaction product identifying osteoclasts is red. $n = 4$ mice per group. Magnification, ×40. $^{*}P < 0.001$ compared with serum (+); $^{\#}P < 0.001$ compared with serum (–).

rect mediators of inflammatory osteolysis prompted us to ask if their participation in this disorder reflects additional osteoclastogenic cytokines, such as M-CSF, which may also represent therapeutic targets. M-CSF mediates survival and proliferation of macrophage precursors and their differentiation into mature phagocytes (17). Given the ontogeny of the osteoclast, it is not surprising that the cytokine also plays an important role in the maturation and survival of this cell. M-CSF also impacts the mature osteoclast by promoting organization of its cytoskeleton (16). The *op/op* mouse in particular underscores the central role the cytokine plays in the osteoclastogenic process. This animal, which bears a point mutation in the *Csf1* gene coding for M-CSF, is born osteopetrotic due to failure to generate osteoclasts and is rescued by the cytokine (22). The transmembrane tyrosine kinase, c-Fms, is the sole M-CSF receptor (23, 24), and deletion of its gene leads to the same phenotype as the *op/op* mouse (25).

While M-CSF is constitutively produced by a range of mesenchymal cells, its regulated secretion has pathological consequences in the context of the osteoclast. Thus, absence of estrogen, the cause of postmenopausal osteoporosis, is due to enhanced bone resorption caused at least in part by increased production of M-CSF by BM stromal cells (26). Similarly, the enhanced osteoclastogenesis attending deletion of the β3 integrin gene is due to stimulated M-CSF expression (16). As regards inflammatory osteolysis, the cytokine is increased in the serum of patients with rheumatoid arthritis (27) and those with severe ankylosing spondylitis (28) as well as in synovial fluid around loose joint prostheses (29). Taken together, these observations suggest that stromal cell–produced M-CSF may be an important mediator of TNF-stimulated osteoclastogenesis. In fact, we find that TNF-α induced M-CSF gene expression in vivo and did so only in the presence of stromal cell–residing TNFRs. The capacity of TNF-α to increase osteoclast precursor numbers, in vivo, is in keeping with the proproliferative and prosurvival properties of abundant M-CSF.

IL-1, whose expression by BMMs and stromal cells is also enhanced by TNF-α, mediates approximately 50% of the osteoclastogenic capacity of TNF-α (18). IL-1, however, does not participate in TNF-induced M-CSF production. Specifically, arrest of IL-1 signaling by either IL-1Ra or deletion of the functional IL-1 receptor has no effect on the capacity of TNF-α to promote M-CSF production or to increase osteoclast precursor number in vitro and in vivo. Thus, M-CSF appears to be a mediator of that component of TNF-stimulated osteoclastogenesis occurring in an IL-1–independent manner.

The development of models of inflammatory arthritis in the context of TNFR chimeric mice enables us to attribute various components of the disease, including synovitis and periarticular osteolysis,

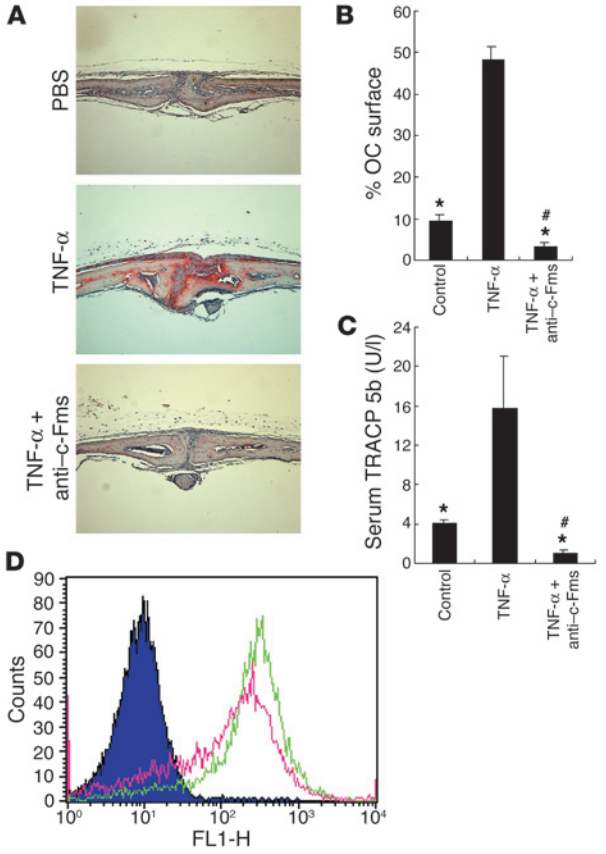

Figure 10

Anti–c-Fms mAb blocks TNF-α–induced osteoclastogenesis and bone resorption in vivo. (**A**) Histological sections of calvariae excised from mice after 5 daily supracalvarial injections of TNF-α, with or without intraperitoneal injection of anti–c-Fms mAb, were stained for TRAP activity (red reaction product). Magnification, ×40. (**B**) The percentage of bone/BM interface covered by osteoclasts was histomorphometrically determined. (**C**) Circulating TRACP 5b levels were determined by ELISA. (**D**) Abundance of CD11b-positive osteoclast precursors in BM recovered from TNF-injected mice with (red line) or without (green line) anti–c-Fms mAb. The black line represents FITC-conjugated isotype mAb. The illustration is representative of 4 separate experiments. $n = 4$ in all groups. $^{*}P < 0.001$ compared with TNF-α alone; $^{\#}P < 0.001$ compared with control.

to specific cell types. We previously noted that osteoclastogenesis induced by relatively modest levels of TNF-α requires TNF-responsive stromal cells (15). On the other hand, an abundance of the cytokine, as obtains in inflammatory osteolysis, is capable of inducing maximal osteoclastogenesis by directly targeting only osteoclast precursors in the presence of constitutive levels of RANKL (10, 15). In this study, we show that the reciprocal is also true. Thus, mice bearing TNFRs on stromal cells, but not osteoclast precursors, optimize inflammation-induced osteoclast recruitment. These observations indicate that in situations of abundant TNF expression, such as rheumatoid arthritis, the cytokine's effect is maximized by targeting either the osteoclast precursor or the stromal compartment. The fact that TNF-α enhances osteoclast precursor number in the presence of only constitutive levels of M-CSF suggests that, like its interaction with RANKL, the inflammatory cytokine synergizes with M-CSF to enhance osteoclast precursor number.

These data, taken in concert, indicate that M-CSF is yet another cytokine playing a central role in inflammatory osteolysis and might be a therapeutic target. M-CSF, however, accelerates formation of osteoclasts by increasing their precursor pool, the majority of which does not become bone resorptive polykaryons, but host defense mononuclear phagocytes. Thus, the coincident immunosuppressive effect of inhibiting macrophage proliferation and survival as a means of arresting inflammatory periarticular erosion is a potential limitation of M-CSF blockade. On the other hand, anti–c-Fms mAb prevents RANKL and M-CSF–induced osteoclast formation at a concentration at least 1 order of magnitude less than its capacity to decrease cell number in vitro. This observation raises the possibility that, in the context of inflammatory osteolysis, osteoclast recruitment is more sensitive to M-CSF inhibition than is macrophage proliferation and/or survival. In fact, mice treated with carrier or anti–c-Fms mAb developed equivalent periarticular inflammation while those receiving the antibody were completely free of pathological osteoclastogenesis and bone resorption. This observation reflects to a substantial degree arrest of TNF signaling, as similar results obtained in TNF-α–injected mice also receiving anti–c-Fms mAb. Like arthritic animals, those directly receiving TNF-α experienced complete arrest of osteoclastogenesis but only a modest decrease in macrophage number. Interestingly, nonpathological osteoclastogenesis located distant from the inflamed joint was robust in each case. While the enhanced sensitivity to c-Fms arrest of pathological, as compared with physiological, osteoclastogenesis remains unexplained, it may reflect participation of redundant cytokines. For example, the osteopetrosis and arrested osteoclastogenesis of the M-CSF–deficient *op/op* mouse resolves with age due to expression of VEGF (30), GM-CSF, and/or IL-3 (31). While speculative, the possibility remains that these 2 cytokines substitute for M-CSF in a physiological setting of osteoclast recruitment.

Thus, M-CSF joins the panoply of cytokines involved in the pathogenesis of inflammatory osteolysis. Although this study represents short-term arrest of M-CSF signaling initiated at induction of the arthritic process, the profundity of its effect on osteoclasts as compared with macrophages enhances its therapeutic appeal. The potential of M-CSF inhibition as a means of treating rheumatoid arthritis is underscored by the development of c-Fms–selective small molecules (32) and the capacity of the tyrosine kinase inhibitor drug Imatinib to target the receptor (33). Given the significant complications encountered with other forms of anticytokine therapy, however, the therapeutic targeting of M-CSF must be approached with caution (34).

Methods

Mice. C57BL/6 mice deleted of genes coding for both TNFR type 1 and TNFR type 2 on a C57BL/6 background were generated as described (15). C57BL/6 WT mice were purchased from the Jackson Laboratory. Animals were housed in the animal care unit of the Department of Pathology, Washington University School of Medicine, and were maintained according to the guidelines of the Association for Assessment of Laboratory Animal Care. All animal experimentation was approved by the Animal Studies Committee of Washington University School of Medicine.

Reagents. The following mAbs were obtained from BD Biosciences: purified rat anti-mouse VCAM-1 (no. 553330), purified rat anti-mouse CD3 molecular complex (no. 555273), FITC-conjugated rat anti-mouse CD11b (no. 553310), purified hamster anti-mouse TNFR1 (no. 559915), PE-conjugated hamster anti-mouse TNFR2 (no. 550086), and isotype control antibodies.

Goat anti-rat IgG microbeads for immunopurification were obtained from Miltenyi Biotec. Recombinant murine TNF-α was prepared in our laboratory as described (15). Recombinant human M-CSF was generously provided by Daved H. Fremont (Washington University, St. Louis, Missouri, USA). Murine RANKL was expressed in our laboratory as described (10).

BM transplantation. Mice were killed by CO_2 gas, and femoral BM cells were flushed with culture medium as described (35). VCAM-1 and CD3-positive cells were depleted from BM by negative selection using MACS goat anti-rat IgG Microbeads (Miltenyi Biotec) as described (15). One day after administration of 10 Gy of total body γ-irradiation, we injected 1×10^6 CD3 and VCAM-1 depleted BM cells in 100 μl PBS into 4- to 6-week-old male mice via tail vein.

In vivo T cell depletion. Female ICR-SCID mice (Taconic) were primed by intraperitoneal injection of 0.5 ml of incomplete Freund's adjuvant. After 7 days, the mice received intraperitoneal injections of 5×10^6 YTS cells, which secrete anti-CD4 antibodies, or H35 cells, which secrete anti-CD8 antibodies (kindly provided by Osami Kanagawa, Washington University, St. Louis, Missouri, USA). One to 2 weeks later, ascites was recovered, incubated at 37°C for 1 hour, and transferred to 4°C overnight. Cells and oil were removed by centrifugation, and ascites was stored at –80°C. Mice were administered 4 weekly injections of 50 μl of anti-CD4 and anti-CD8 ascites to assure arrest of T cell generation in vivo (15).

FACS analysis. To assess the number of osteoclast precursors, freshly isolated BM cells were incubated in NaN_3 (0.1%) plus FBS-PBS (FBS, 1%) for 30 minutes with FITC-conjugated rat anti-mouse CD11b mAb. The samples were diluted with the same solution and analyzed by FACS for CD11b-expressing cells. To evaluate BM engraftment, BMMs were incubated for 30 minutes with anti-TNFR1 mAb and then for 30 minutes with FITC-conjugated anti-IgG mAb. They were then washed and diluted with NaN_3 plus FBS. A second aliquot of BM cells was incubated for 30 minutes with PE-labeled anti-TNFR2 mAb. TNFR1 and TNFR2 expression were analyzed by FACS.

RNA preparation and RT-PCR analysis. Total RNA from BM cells was isolated by RNeasy mini kit (QIAGEN). For RT-PCR analysis, cDNA was synthesized from 1 μg of total RNA using reverse transcriptase and oligo-dT primers in a volume of 20 μl. PCR was performed with a cDNA reaction mixture using PCR supermix (Invitrogen Corp.) and appropriate primers in a volume of 50 μl. The following primers were used: GAPDH, 5′-ACTTTGTCAAGCTCATTTCC-3′ and 5′-TGCAGCGAACTTTATTGATG-3′; RANK, mouse RANK PCR Primer Pair (R&D Systems); RANKL, human/mouse TRANCE/TNFSF11 PCR Primer Pair (R&D Systems.); and M-CSF, 5′-GACTTCATGCCAGATTGCC-3′ and 5′-GGTGGCTTTAGGGTACAGG-3′. Samples were transferred to a programmable thermal cycler (Hybaid; Thermo Electron Corporation) preheated to 94°C. Each cycle consisted of a denaturation step at 94°C for 45 seconds, an annealing step at 55°C for 45 seconds, and an extension step at 72°C for 45 seconds for RANKL, RANK, and GAPDH and a denaturation step at 94°C for 1 minute, an annealing step at 58°C for 1 minute, and an extension step at 72°C for 1 minute for M-CSF. We separated 10-μl aliquots of PCR products by electrophoresis on a 2.0% agarose gel.

Serum transfer arthritis. KRN-TCR transgenic mice on a C57BL/6 background were kindly provided by D. Mathis and C. Benoist (Harvard University Medical School, Boston, Massachusetts, USA). K/BxN mice, which spontaneously develop severe inflammatory arthritis (18) and whose serum immunoglobulin is arthrogenic in a T cell–independent manner (15), in mouse strains other than KRN, were generated by breeding KRN-TCR with nonobese diabetic mice (Taconic). Serum was obtained from 6- to 12-week-old K/BxN mice, pooled, and stored in aliquots at –70°C. T cell–depleted WT to WT, WT to KO, KO to WT, and KO to KO mice were injected once intraperitoneally with 200 μl of serum or PBS. Paw thickness was measured with a caliper daily for 10 days. A second group of animals was sacrificed at day 7 for histology and FACS analysis. Paws were stripped of soft tissue, and bones and joints were subjected to histological examination and evaluation of numbers of CD11b-positive cells.

Administration of anti–c-Fms antibody. AFS98, a rat monoclonal, anti-murine c-Fms antibody (IgG2a) that inhibits M-CSF–dependent colony formation and cell growth by blocking the binding of M-CSF to its receptor, has been described (21). The AFS98 hybridoma was kindly supplied by Shin-Ichi Nishikawa (Graduate School of Medicine, Kyoto University Medical School, Kyoto, Japan). The clone was maintained in HyQ-CCM1 medium (HyClone), and the antibody was purified using Protein G (Sigma-Aldrich). We administered intraperitoneally 500 μm of AFS98 in 500 μl of PBS or PBS alone every day for 7 days to arthritic or TNF-injected mice.

Macrophage proliferation assay. BMMs from WT mice were cultured with several doses of AFS98 mAb in the presence of 100 ng/ml M-CSF. After 3 days, the number of viable cells was measured using the MTT (3-[4,5-dimethylthiazol-2yl]-2,5-diphenyltetrazoliun bromide; Sigma-Aldrich) assay. In brief, 10 μl MTT (5 mg/ml) was added to 100 μl culture medium in each well and incubated at 37°C for 4 hours. We added 150 μl 0.04N HCl in isopropanol to each well to stop the reaction, and MTT absorbance was determined at OD of 570 nm.

Serum TRACP 5b assay. Serum was obtained 7 days after injection of arthrogenic serum or following 5 days of daily TNF-α administration. TRACP 5b levels were determined according to the protocol of the MouseTRAP Assay kit (IDS).

Histological analysis. Osteoclast number was determined using the Osteomeasure System version 2.2 (Osteometrics Corp.).

Statistics. All data are expressed as mean ± SD. Statistical significance was calculated by 2-tailed Student's *t* test.

Acknowledgments

This work was supported by NIH grants AR032788, AR046523, and AR048853; DK056341 from the Clinical Nutrition Research Unit (to S.L. Teitelbaum); and AR046852 and AR048812 (to F.P. Ross).

Received for publication July 1, 2005, and accepted in revised form September 23, 2005.

Address correspondence to: Steven L. Teitelbaum, Washington University School of Medicine, Department of Pathology and Immunology, Campus Box 8118, 660 South Euclid Avenue, St. Louis, Missouri 63110, USA. Phone: (314) 454-8463; Fax: (314) 454-5505; E-mail: teitelbs@wustl.edu.

1. Udagawa, N., et al. 1990. Origin of osteoclasts: mature monocytes and macrophages are capable of differentiating into osteoclasts under a suitable microenvironment prepared by bone marrow-derived stromal cells. *Proc. Natl. Acad. Sci. U. S. A.* **87**:7260–7264.
2. Lacey, D.L., et al. 1998. Osteoprotegerin ligand is a cytokine that regulates osteoclast differentiation and activation. *Cell.* **93**:165–176.
3. Yasuda, H., et al. 1998. Osteoclast differentiation factor is a ligand for osteoprotegerin/osteoclastogenesis-inhibitory factor and is identical to TRANCE/RANKL. *Proc. Natl. Acad. Sci. U. S. A.* **95**:3597–3602.
4. Bekker, P.J., et al. 2004. A single-dose placebo-controlled study of AMG 162, a fully human monoclonal antibody to RANKL, in postmenopausal women. *J. Bone Miner. Res.* **19**:1059–1066.
5. Feldmann, M., and Maini, R.N. 2001. Anti-TNF therapy of rheumatoid arthritis: what have we learned? *Ann. Rev. Immunol.* **19**:163–196.
6. Gravallese, E.M. 2002. Bone destruction in arthritis. *Ann. Rheum. Dis.* **61**:84–86.
7. Romas, E., Gillespie, M.T., and Martin, T.J. 2002. Involvement of receptor activator of NFkappaB ligand and tumor necrosis factor-alpha in bone destruction in rheumatoid arthritis. *Bone.* **30**:340–346.
8. Redlich, K., et al. 2002. Osteoclasts are essential for TNF-α-mediated joint destruction. *J. Clin. Invest.* **110**:1419–1427. doi:10.1172/JCI200215582.

9. Ritchlin, C.T., Haas-Smith, S.A., Li, P., Hicks, D.G., and Schwarz, E.M. 2003. Mechanisms of TNF-α- and RANKL-mediated osteoclastogenesis and bone resorption in psoriatic arthritis. *J. Clin. Invest.* **111**:821–831. doi:10.1172/JCI200316069.
10. Lam, J., et al. 2000. TNF-α induces osteoclastogenesis by direct stimulation of macrophages exposed to permissive levels of RANK ligand. *J. Clin. Invest.* **106**:1481–1488.
11. Kong, Y.Y., et al. 1999. Activated T cells regulate bone loss and joint destruction in adjuvant arthritis through osteoprotegerin ligand. *Nature.* **402**:304–309.
12. Li, J., et al. 2000. RANK is the intrinsic hematopoietic cell surface receptor that controls osteoclastogenesis and regulation of bone mass and calcium metabolism. *Proc. Natl. Acad. Sci. U. S. A.* **97**:1566–1571.
13. Smolen, J.S., and Steiner, G. 2003. Therapeutic strategies for rheumatoid arthritis. *Nat. Rev. Drug Discov.* **2**:473–488.
14. Zwerina, J., et al. 2004. Single and combined inhibition of tumor necrosis factor, interleukin-1, and RANKL pathways in tumor necrosis factor-induced arthritis: effects on synovial inflammation, bone erosion, and cartilage destruction. *Arthritis Rheum.* **50**:277–290.
15. Kitaura, H., et al. 2004. Marrow stromal cells and osteoclast precursors differentially contribute to TNF-α induced osteoclastogenesis in vivo. *J. Immunol.* **173**:4838–4846.
16. Faccio, R., Zallone, A., Ross, F.P., and Teitelbaum, S.L. 2003. c-Fms and the αvβ3 integrin collaborate during osteoclast differentiation. *J. Clin. Invest.* **111**:749–758. doi:10.1172/JCI200316924.
17. Lotze, M.T., and Hamilton, J.A. 2003. Macrophage colony stimulating factor [CSF-1]. In *The cytokine handbook*. A.W. Thomson and M.T. Lotze, editors. Elsevier Science Ltd. London, United Kingdom. 545–573.
18. Wei, S., Kitaura, H., Zhou, P., Ross, F.P., and Teitelbaum, S.L. 2005. IL-1 mediates TNF-induced osteoclastogenesis. *J. Clin. Invest.* **115**:282–290. doi:10.1172/JCI200523394.
19. Kouskoff, V., et al. 1996. Organ-specific disease provoked by systemic autoimmunity. *Cell.* **87**:811–822.
20. Korganow, A., et al. 1999. From systemic T cell self-reactivity to organ-specific autoimmune disease via immunoglobulins. *Immunity.* **10**:451–461.
21. Sudo, T., et al. 1995. Functional hierarchy of c-kit and c-fms in intramarrow production of CFU-M. *Oncogene.* **11**:2469–2476.
22. Wiktor-Jedrzejczak, W., et al. 1990. Total absence of colony-stimulating factor 1 in the macrophage-deficient osteopetrotic (op/op) mouse. *Proc. Natl. Acad. Sci. U. S. A.* **87**:4828–4832.
23. Sherr, C.J., Matsushime, H., and Roussel, M.F. 1992. Regulation of CYL/cyclin D genes by colony-stimulating factor 1. *CIBA Found. Symp.* **170**:209–219.
24. Stanley, E.R., et al. 1997. Biology and action of colony-stimulating factor-1. *Mol. Reprod. Dev.* **46**:4–10.
25. Dai, X.-M., et al. 2002. Targeted disruption of the mouse colony-stimulating factor 1 receptor gene results in osteopetrosis, mononuclear phagocyte deficiency, increased primitive progenitor cell frequencies, and reproductive defects. *Blood.* **99**:111–120.
26. Srivastava, S., et al. 1998. Estrogen blocks M-CSF gene expression and osteoclast formation by regulating phosphorylation of Egr-1 and its interaction with Sp-1. *J. Clin. Invest.* **102**:1850–1859.
27. Kawaji, H., Yokomura, K., Kikuchi, K., Somoto, Y., and Shirai, Y. 1995. Macrophage colony-stimulating factor in patients with rheumatoid arthritis [In Japanese]. *Nippon Ika Daigaku Zasshi.* **62**:260–270.
28. Yang, C., et al. 2004. Serum levels of matrix metalloproteinase 3 and macrophage colony-stimulating factor 1 correlate with disease activity in ankylosing spondylitis. *Arthritis Rheum.* **51**:691–699.
29. Takei, I., et al. 2000. High macrophage-colony stimulating factor levels in synovial fluid of loose artificial hip joints. *J. Rheumatol.* **27**:894–899.
30. Niida, S., et al. 1999. Vascular endothelial growth factor can substitute for macrophage colony-stimulating factor in the support of osteoclastic bone resorption. *J. Exp. Med.* **190**:293–298.
31. Myint, Y.Y., et al. 1999. Granulocyte/macrophage colony-stimulating factor and interleukin-3 correct osteopetrosis in mice with osteopetrosis mutation. *Am. J. Pathol.* **154**:553–566.
32. Murray, L.J., et al. 2003. SU11248 inhibits tumor growth and CSF-1R-dependent osteolysis in an experimental breast cancer bone metastasis model. *Clin. Exp. Metastasis.* **20**:757–766.
33. Dewar, A.L., Zannettino, A.C., Hughes, T.P., and Lyons, A.B. 2005. Inhibition of c-fms by imatinib: expanding the spectrum of treatment. *Cell Cycle.* **4**:851–853.
34. Genovese, M.C., et al. 2004. Combination therapy with etanercept and anakinra in the treatment of patients with rheumatoid arthritis who have been treated unsuccessfully with methotrexate. *Arthritis Rheum.* **50**:1412–1419.
35. Abu-Amer, Y., et al. 2000. Tumor necrosis factor receptors types 1 and 2 differentially regulate osteoclastogenesis. *J. Biol. Chem.* **275**:27307–27310.